

Chemical induced delithiation on Li_xMnPO_4 : an investigation about the phase structure

Melanie Köntje

ZSW (Zentrum für Sonnenenergie- und Wasserstoff-
Forschung, Baden-Württemberg),
Helmholtzstrasse 8, 89081 Ulm, Germany

Giorgia Greco¹

Helmholtz-Zentrum Berlin für Materialien und Energie
GmbH, Hahn-Meitner-Platz 1, D-14109 Berlin, Germany.
giorgia.greco@helmholtz-berlin.de

Giuliana Aquilanti

ELETTRA-Sincrotrone Trieste,
34149 Basovizza (TS), Italy
giuliana.aquilanti@elettra.eu

Luca Olivi

ELETTRA-Sincrotrone Trieste,
34149 Basovizza (TS), Italy
luca.olivi@elettra.ue

Peter Axmann

ZSW (Zentrum für Sonnenenergie- und Wasserstoff-
Forschung, Baden-Württemberg),
Helmholtzstrasse 8, 89081 Ulm, Germany
peter.axmann@zsw-bw.de

Margret Wohlfahrt-Mehrens

ZSW (Zentrum für Sonnenenergie- und Wasserstoff-
Forschung, Baden-Württemberg),
margret.wohlfahrt-mehrens@zsw-bw.de

¹ Corresponding author

ABSTRACT

Understanding the $\text{LiMnPO}_4/\text{MnPO}_4$ phase transition is of great interest in order to further improve the electrochemical performance of this cathode material. Since most of the previously published literature deals with characterization of chemically delithiated Li_xMnPO_4 , the aim of this study is to compare and study the composition and structure of the different phases that are generated upon chemical delithiation of Li_xMnPO_4 . Bare and carbon-coated lithium manganese phosphates are prepared via a combined coprecipitation-calcination method. Partial delithiation to two different degrees of delithiation Li_xMnPO_4 ($x = 0.24/0.23$ and 0.45) for carbon-coated and/or bare materials is achieved using an excess of nitronium tetrafluoroborate in acetonitrile. The effect of carbon-coating has been also considered. Standard materials characterization with XRD (X-Ray Diffraction) and ICP-OES (Inductive Coupled Plasma spectrometry and Optical Emission Spectroscopy) analysis are in accordance with literature data, but further cerimetric analysis revealed serious deviations, showing differences in the degree of delithiation to the average degree of oxidation. A structural characterization of the atomic and electronic local structure of the materials is also obtained using XAS (X-ray Absorption Spectroscopy) technique.

Keywords

Energy storage, High Voltage Cathodes, Phase Transition, XRD, XAFS, Phospho Olivines, Batteries, Chemical Delithiation.

1. INTRODUCTION

Transition metal phospho olivines turned out to be a promising alternative to the commonly used layered oxides since Padhi et al. first reported about the electrochemical performance of LiFePO_4 as possible cathode material [16]. In comparison to the commonly used commercialized layered oxides phospho olivines provide a low toxicity- environmental benignity, higher potentials (3.45 V vs. Li/Li^+ for LiFePO_4 , 4.1 V vs. Li/Li^+ for LiMnPO_4) [21, 23] and thermal stability [24]. Many efforts have been made to investigate the electrochemical de-/ intercalation of lithium ions into the LiFePO_4 host pronouncing a first-order heterogeneous two phase transition [16, 20, 18]. For the promising lithium manganese phospho olivine the phase transition has not been investigated in such detail, but the $\text{LiMnPO}_4/\text{MnPO}_4$ transition is announced to proceed in an equivalent heterogeneous two phase transition as investigated for the iron analogue [2, 5]. The lower electrochemical performance in comparison to the iron analogue is commonly addressed to the inactivated $\text{Mn}^{2+}/\text{Mn}^{3+}$ redox reaction. This phenomenon has been mostly explained by a lower electronic and ionic conductivity, interface strain at the $\text{LiMnPO}_4/\text{MnPO}_4$

phase boundary and local distortions due to the Jahn-Teller-ion Mn^{3+} [23, 15, 4, 17]. Reporting detailed information about the phase composition, the $\text{Li}_x(\text{Mn}_y\text{Fe}_{1-y})\text{PO}_4$ ($0 \leq x \leq 1$) phase diagram first published by Yamada et al. [25] shows distinct regions of solid solutions and two phase regimes. Further detailed structural investigations of the partly delithiated Li_xMnPO_4 materials pointed out effects due to differences in the electronic states of $\text{Mn}^{3+}\text{-O}_6$ and $\text{Fe}^{3+}\text{-O}_6$ which cause the Jahn-Teller distortion for Mn^{3+} . In the present paper we aim to evaluate and compare the composition of the different phases that generate upon chemical delithiation of the Li_xMnPO_4 .

For the purpose to characterize these products we used a number of spectroscopic and analytical techniques. XRD and ICP-OES analysis turned out to well agree with previously published literature. Additionally we took advantages of cerimetric analysis, a powerful technique that helped to gain further details on the oxidation state of Mn. We show severe differences for the average degree of oxidation measured by cerimetry to the calculated value from ICP-OES analysis. Furthermore a XAS analysis has been performed, allowing us a full structural characterization including information about oxygen bonding and valence state.

2. EXPERIMENTAL

2.1 Sample Preparation

Synthesis of the carbon-coated and non carbon-coated lithium manganese phospho olivines were performed via a combined coprecipitation calcination route. The precursor was obtained from appropriate aqueous solutions containing the metal salts in certain molar ratios. Annealing the precursor in an inert atmosphere resulted in the desired LiMnPO_4 phospho olivines. For the carbon coating appropriate organic carbon containing solid substances were introduced to the precursor and properly mixed before annealing. The amount therefore has been calculated to obtain 5wt% carbon relative to the amount of manganese on the LMPO/C. Chemical delithiation of the bare and uncoated LiMnPO_4 has been achieved by applying excess nitroniumtetrafluoroborate in acetonitrile (4:1 relative to the amount of Mn(II)), dry reaction conditions, inert gas, elevated temperature (40°C) under kinetic reaction control. To stop the delithiation process the LMPO/C material has been separated from the delithiation agents, accurately washed and dried. Reaction duration of 29min ($\text{Li}_0.45\text{MnPO}_4/\text{C}$), 90min ($\text{Li}_0.24\text{MnPO}_4/\text{C}$) and 21min ($\text{Li}_0.23\text{MnPO}_4$) have been applied. Mn(II) was determined by cerimetry and thus the conversion Mn(II) to Mn(III) calculated. A Methrom Titrino titration system has been used. A more detailed description is reported elsewhere [1]. We have obtained the materials listed below.

Carbon coated samples:

LiMnPO_4 labeled as LMPO/C;

$\text{Li}_{0.45}\text{MnPO}_4$ labeled as LMPO-0.5/C;

$\text{Li}_{0.24}\text{MnPO}_4$ labeled as LMPO-0.2/C;

Uncoated sample:

$\text{Li}_{0.23}\text{MnPO}_4$ labeled as LMPO-0.2.

3. RESULTS AND DISCUSSION

3.1 Chemical delithiation procedure of LMPO

Since pure Li_xMnPO_4 powders could be easily obtained via several chemical delithiation procedures [25, 13] these materials have been often investigated for detailed examinations of the $\text{LiMPO}_4/\text{MPO}_4$ phase transition [24, 2, 25, 13, 12].

The delithiation process as described in the synthesis procedure exhibits significant differences compared to electrochemical delithiation procedures. During electrochemical delithiation the redox process takes place at electrically conducted points at the active materials and additives grains within the electrolyte. The reaction is mainly dependent from charge-transfer characteristics, ion diffusivity and the SEI characteristics of this electrode composition. Contrarily, the chemical delithiation process takes not place within the standard electrolyte environment considering the SEI, but takes place in non-aqueous solution at the complete grain surface. The reaction is expected to directly take place between the active materials grains and the delithiation agents with the lack of SEI characteristics and in changed electrolyte to common standard electrochemical conditions. The obtained chemically delithiated phases are supposed to be not identical to electrochemically delithiated Li_xMnPO_4 as we will show during the material characterization.

3.2 Compositional analysis: degree of oxidation of samples

Firstly, the degree of oxidation of manganese in the pure LMPO/C has been evaluated, thus having a benchmark. The expected calculated value from ICP-OES analysis of 2.00 has been confirmed by cerimetry (2.01), as shown in Fig. 1 ($x = 1$). Contrarily both chemically delithiated carbon-coated Li_xMnPO_4 ($x = 0.45$ and $x = 0.24$) showed lower values in comparison to the calculated degrees of oxidation of manganese. This hence indicates a formal higher amount of “ Mn^{2+} ” concomitant to a lower amount of “ Mn^{3+} ” as already considered. Due to these differences we suppose that the assumption all residual lithium depicts the equivalent amount of Mn^{2+} which crystallises in the olivine structure, is not complete. Thus it should be extended by an amount of amorphous Mn^{2+} containing phosphates with no retaining lithium in the structure. Delithiated $\text{Mn}^{\text{III}}\text{PO}_4$ is known to decompose to manganese(II)pyrophosphate under oxygen release during thermal treatment [2, 12, 3]. The formal Li:Mn:P ratio does not underlie any changes caused by the MnPO_4 to $\text{Mn}_2\text{P}_2\text{O}_7$ transformation.

Subsequently there could not be detected any change in the chemical composition via ICP-OES analysis. During the chemical delithiation process we suppose an equivalent decomposition of the MnPO_4 phase. Since we found a degradation of the material caused by the chemical delithiation procedure we suppose the formation of amorphous Mn^{2+} containing phases not detectable for XRD as reason for the deviations depicted from ICP and cerimetry.

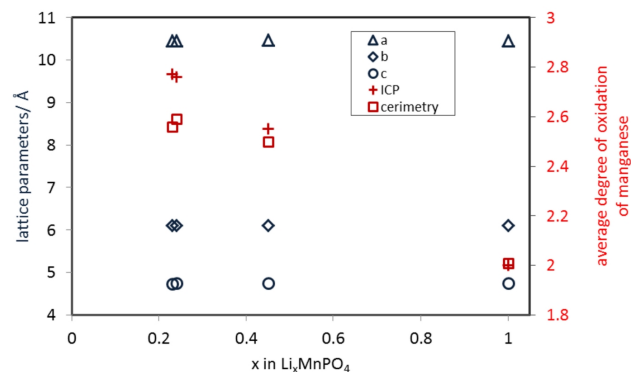


Figure 1: Right scale: comparison of the average degree of oxidation of manganese calculated via ICP-OES analysis and cerimetry for LMPO/C, LMPO-0.2 and LMPO-x/C ($x = 0.5$ and 0.2). Left scale: the x lattice parameters a , b and c (spacegroup $Pnma$) in Å obtained by XRD analysis.

3.3 Structural characterization with XRD technique

The chemical composition was calculated from ICP-OES analysis and normalized to the amount of manganese in LMPO-0.5/C and LMPO-0.2/C. Powder diffraction patterns of LiMnPO_4 carbon-coating starting material LMPO/C and of the chemically delithiated ones are shown in Fig. 2 as well as the non carbon-coated chemically delithiated one (magenta curve).

The X-ray diffraction pattern for the LMPO/C (red curve) shows the peaks of the orthorhombic LiMnPO_4 olivine ($Pnma$). From the quantitative Rietveld analysis, we could determine also a rather low amount of Li_3PO_4 (2.3 wt%). Further quantification of the two phases, LiMnPO_4 and Li_3PO_4 , has been done by ICP-OES chemical analysis, which revealed 97.6 wt% LiMnPO_4 and 2.4 wt% Li_3PO_4 in full accordance with the XRD results. As it can be seen from the X-ray patterns of the chemically delithiated samples (Fig. 2, blue and red curves), an additional phase of MnPO_4 with purpurite structure appears under consumption of LiMnPO_4 . No Li_3PO_4 could be indexed, which we expect to be partially extracted during the chemical delithiation process. Nevertheless phase quantities less than 2 wt% are below the limit of determination via XRD. The delithiation process leads to a broadening of the peaks related to the Li_xMnPO_4 phases. We therefore evaluated the lattice parameters of the remaining lithiated phase (Fig.1) and calculated the crystallite sizes of the carbon-coated Li_xMnPO_4 according to Pawley-fits. All lattice parameters remain un-

changed, showing negligibly higher values with increasing degree of oxidation. Tab 1 reports the comparison of the relevant values obtained. Both chemically delithiated LMPO-x/C ($x = 0.5$ and $x = 0.2$) exhibit a reduction of the crystallite size for the remaining lithiated phase to $\sim 1/2$, and for the new delithiated phase of $\sim 1/3$ compared to the raw material. The results reported until now are in well agreement with previously published literature data [24, 25, 1, 12], where chemically delithiated Li_xMnPO_4 have been obtained via treatment with nitronium tetrafluoroborate.

The influence of the carbon coating has been also evaluated. The carbon coating has been added with the intention of creating an additional protecting and supporting surface layer on the active material considering the electronic conductivity during the redox process as well as the lithium ion diffusion mechanism during the in-/exsertion process. In Fig 2 (upper panel, magenta curve) the diffraction pattern of LMPO-0.2 is shown. It is obvious that the carbon-coating prevents the material of a great amorphization. This might be due to the strongly enhanced reaction rate of delithiation for the non carbon-coated material, as already pointed out in section 2.1.

The XRD results reported in Fig. 2 for the chemically delithiated samples demonstrated the coexistence of a fully lithiated phase (LiMnPO_4) and of a fully delithiated phase (MnPO_4). This would be explained by a heterogeneous two phase transition. Since the Li_xMnPO_4 stoichiometry has been determined on the basis of ICP-OES analysis, and considering that no impurities can be detected from the X-ray patterns, we believe that all the residual lithium-ions reside in the olivine structure. Thus the stoichiometry of $\text{Li}_{0.45}\text{MnPO}_4$ leads to a phase composition of 45 mol%.

LiMnPO_4 and 55 mol% MnPO_4 which refers to an average degree of conversion of 0.55. Similarly, the $\text{Li}_{0.24}\text{MnPO}_4$ material refers to an average degree of conversion of 0.76. From these significant results the average degree of oxidation of manganese has been calculated. The two degrees of conversion of 0.55 and 0.76 lead to the average degrees of oxidation of manganese of 2.55 and 2.76 within the heterogeneous $\text{LiMn}^{\text{II}}\text{PO}_4/\text{Mn}^{\text{III}}\text{PO}_4$ system.

Results from cerimetry show for the non carbon-coated LMPO-0.2 in comparison to the carbon-coated equivalent, even a greater deviation to the calculated value of the average degree of oxidation (Fig. 1). Considering its higher degree of amorphization concomitant to this deviation, we assume for the non carbon-coated material even a higher decomposition of the chemically delithiated MnPO_4 .

Table 1: Crystallite sizes in terms of diameters d obtained by XRD analysis for pristine LMPO/C and chemically delithiated carbon coated samples.

Size d (nm)	LMPO/C	LMPO-0.5/C		LMPO-0.2/C	
	Raw	LiMnPO_4	MnPO_4	LiMnPO_4	MnPO_4
	94 ± 5	51 ± 10	34 ± 10	53 ± 7	29 ± 6

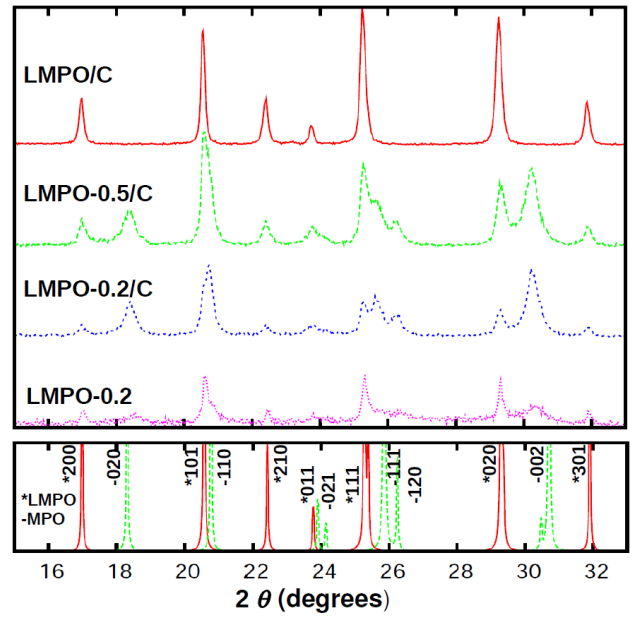


Figure 2: Upper panel: powder diffraction patterns of chemically delithiated LMPO-x/C with carbon-coating ($x = 0.5, 0.2$) and without LMPO-0.2. Lower panel: theoretical diffraction patterns of the lithiated phase of LiMnPO_4 (labeled as LMPO) and completely delithiated phase MnPO_4 (labeled as MPO).

3.4 Local structure investigation with XAS technique

As it is well known, the XAS technique is sensitive to the local atomic structure up to 5-10 Å around photoabsorbing sites, selected by their atomic number, and therefore it is a very useful tool for nanostructural and amorphous materials study [9]. Due to the possibility to extract chemically specific short range information, in combination with XRD it allows a full structural characterization including information about bonding and valence state. Regarding the investigations shown above of the average degree of oxidation of manganese in the following samples LMPO-0.5/C and LMPO-0.2 are investigated more in detail for the following reason. LMPO-0.5/C and LMPO-0.2/C show similar values for the crystallite sizes. The duration of their delithiation processes have been in relation to each other. The deviation of the average degree of oxidation of manganese within the ICP based values and cerimetric results differ for the LMPO-0.2/C more, LMPO-0.5/C are closer. Contrarily, the uncoated LMPO-0.2 suffers from quite high particle size degradation and an even higher deviation between the ICP-OES based values and cerimetry results. From this point of view we aim to focus on LMPO-0.5/C considering its smallest deviations within the evaluation techniques, and the LMPO-0.2 which shows the greatest deviations and material degradation. Combining them enables to give insight

into the effect of the carbon coating first and second the manganese content e.g. its phases composition after a chemical delithiation process.

3.4.1 X-ray Absorption Near Edge Spectroscopy (XANES)

In Fig. 3(a), we report the near-edge XAS spectra of the Mn K-edges of LMPO-0.5/C and LMPO-0.2 after removal of the pre-edge absorption (without normalization to the absorption jump). The amount of Mn quantity is different for the two samples. After the delithiation procedure the amount of Mn in the LMPO-0.2 sample is lower of $\sim 60\%$ respect to the LMPO-0.5/C, but the electronic structure is mainly the same for the different delithiated samples as shown in Figure 3(b) by the direct comparison between the normalized near-edge XAS spectra. This is also confirmed by the XANES of the Mn K-edge pre-edge position proper of the second order $1s-3d$ transition shown in Fig. 4. The pre-edge and the Mn K-edge positions are first qualitative indicators of the valence of manganese [19, 11]. For both LMPO-0.5/C and LMPO-0.2 a similar valence state between II and III can be confirmed. Moreover, looking at Fig. 4 a slight shift of the absorption maximum towards higher energy and an increase of intensity are indices for a slight increase of the Mn valence state for the more delithiated sample LMPO-0.2. Comparing this result with the above described compositional analysis, it can be seen that the mean increased degree of oxidation of manganese for the LMPO-0.2 sample evaluated by ICP-OES analysis and cerimetry is confirmed by XAS analysis. It should be noted that there is no mean difference in the Mn K-edge position for the two samples.

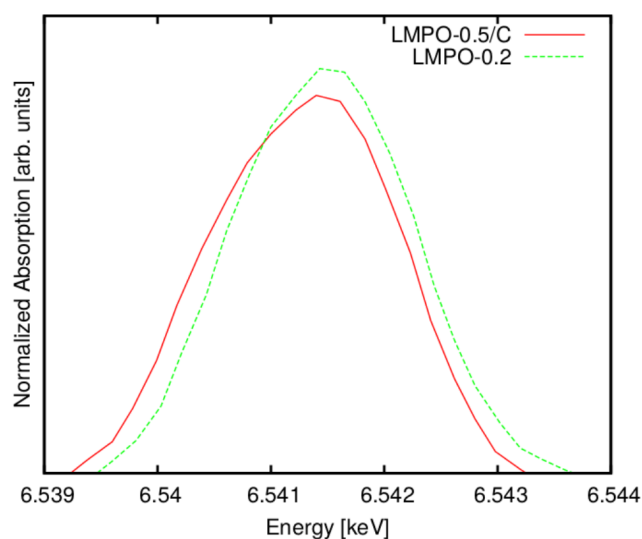


Figure 4: Normalized Mn pre-edge feature of the two samples with different delithiation state.

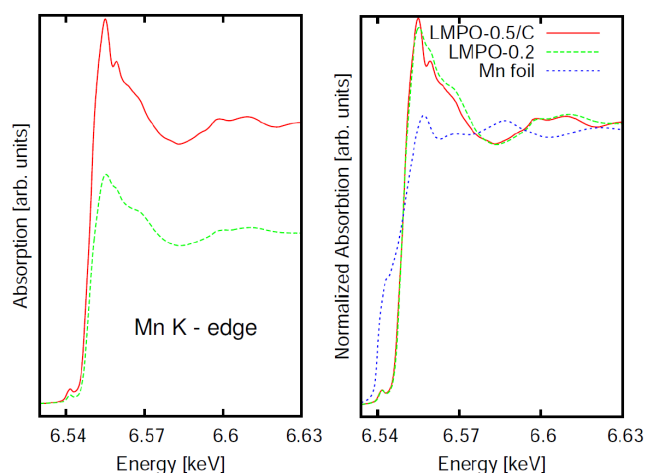


Figure 3: (a) Comparison of XANES Mn K-edge spectra of LMPO/C with different delithiation state powder, (b) the XANES normalized spectra of the samples are compared with the Mn foil at K - edge

3.4.2 X-ray Absorption Near Edge Spectroscopy (XANES)

The LMPO-0.5/C and LMPO-0.2 extracted EXAFS signals and the moduli of their Fourier Transforms (normalized) are compared in Fig. 5 and first shell fitting is shown in Fig. 6, while first shell detailed results of GNXAS structural refinements are presented in Tab 2. Looking at EXAFS signals at Fig. 5 upper panel, the difference in the intensity is evident, due to the mainly amorphous nature of the LMPO-0.2 sample. Looking at the normalized moduli of the Fourier Transforms (Fig. 5, bottom panel) the LMPO-0.2 intensity of further shells signals appear less intense indicating in this sample only a short range order. Three different Mn-O distances were found for LMPO-0.5/C and LMPO-0.2 (Fig. 6) in agreement with crystallographic and vibrational data [6] and lattice parameters obtained by XRD. The delithiated phase $Mn^{3+}PO_4$ (here mentioned as MPO) could be fitted with two different Mn-O distances of coordination number 4 (square planar) and 2 (vertical arrangement). This clearly shows the non-uniform $Mn^{3+}-O_6$ environment due to the Jahn-Teller distortion. For the residual fully lithiated $LiMnPO_4$ (LMPO) phase EXAFS analysis shows only one Mn-O distance indicating an uniform Mn-O coordination in the $Mn^{2+}-O_6$ coordination polyhedral. The more delithiated LMPO-0.2 sample shows an equivalent EXAFS analysis with three Mn-O distances correlated to the $Mn^{3+}-O_6$ and $Mn^{2+}-O_6$ polyhedra. But a Mn-O (I) contraction and increasing structural disorder (Debye-Waller parameter) could be obtained (see Fig. 6 and Tab. 2).

The deviations to smaller values in comparison to literature data still needs to be further worked on. Also the different behavior of the Mn-O (I) and Mn-O (II) distances should be further investigated. This could be further discussed in light of the assumed formation of amorphous Mn^{2+} containing phases.

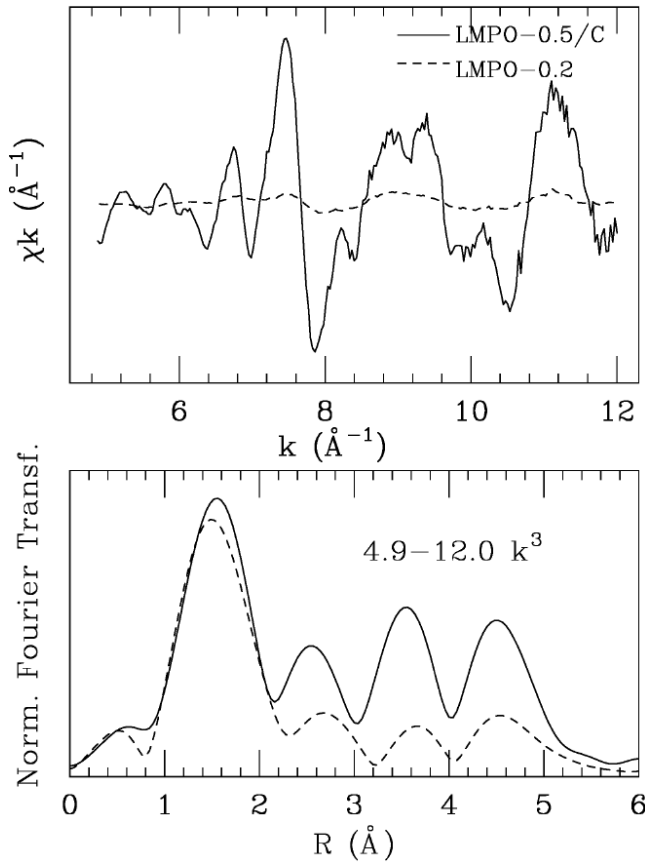


Figure 5: Mn K-edge EXAFS spectra (after background subtraction, k weighted) (top) and Fourier Transforms (FT) (bottom) for LMPO-0.5 solid line, LMPO-0.2 dashed line.

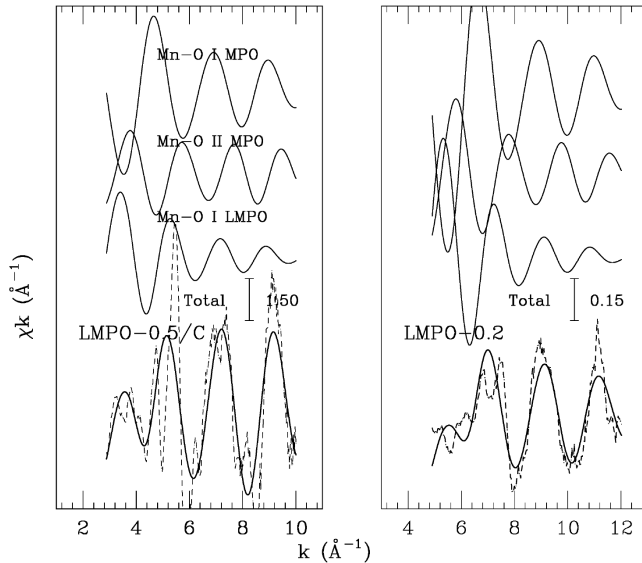


Figure 6: The best fit results of GNXAS analysis performed for LMPO-0.5/C and LMPO-0.2 Mn K-edge (k^3 weighted).

Upper curves represent components of the model signal: Mn-O total two-body signal for the LMPO/C and MPO phases.

4. CONCLUSIONS

The above shown investigations aim to clarify the conformity of chemically and electrochemically delithiated $\text{Li}_x \text{MnPO}_4$. Experimental values from cerimetric analysis gave reasons to out doubts about the direct comparability of chemically and electrochemically delithiated $\text{Li}_x \text{MnPO}_4$. The lower average degree of oxidation examined by cerimetry leads to the assumption of decomposition of the delithiated phase MnPO_4 and formation of amorphous $\text{Mn}_2\text{P}_2\text{O}_7$ or generally spoken Mn^{2+} -containing amorphous phosphorous rich phases during the chemical delithiation process since no other crystalline phases are apparent in XRD analysis. High-quality XAS spectra at the Mn K-edge of the LMPO-0.5/C and LMPO-0.2 were show the presence of amorphous $\text{Mn}_2\text{P}_2\text{O}_7$ can be by the XANES pre-peak shape and position and by a deeper EXAFS analysis evaluating the signal contribution proper of the $\text{Mn}_2\text{P}_2\text{O}_7$ phase. From XANES and EXAFS analysis confirmed valence states between II and III, in agreement with to cerimetry. Moreover LMPO-0.2 sample shows a lower content of Mn respect to the less delithiated LMPO-0.5/C. During the delithiation process the 60% of Mn is lost due to the solubility of Mn^{2+} . A weak short range order indicating the strong material grinding and amorphization for LMPO-0.2 was shown. From first shell fitting first detailed results of GNXAS structural refinements have been presented. For both investigated samples a strong Jahn-Teller distortion, proper of the delithiated phase, has been detected. Deviations of the bond lengths from literature still need further investigations facing the expected decomposition of MnPO_4 . Furthermore, facing XRD and ICP-OES analysis additional characterization techniques like cerimetry would be proposed. The obtained results will be used in our future works.

Table 2: Structural parameters obtained by GNXAS analysis: R_{fit} [Å] - the average inter-atomic distance, σ^2 [10^{-3}Å^2] - the standard deviation of distance, the N_x ($x=\text{cal}$ and tot) - is the obtained and total coordination number respectively. R_{model} [Å] is the expected interatomic distance

	bond I-shell	R_{model}	R_{fit}	σ^2	N_{cal}
LMPO-0.5/C:					
(1-x) MnPO_4	Mn-O I	1.95	1.88(5)	8.0(1)	4*
(1-x) MnPO_4	Mn-O II	2.08	2.07(3)	3.0(1)	2*
x LiMnPO_4	Mn-O I	2.22	2.17(5)	10(5)	6
LMPO-0.2:					
(1-x) MnPO_4	Mn-O I	1.95	1.85(2)	5.7(5)	4*
(1-x) MnPO_4	Mn-O II	2.08	2.05(3)	3.0(1)	2*
x LiMnPO_4	Mn-O I	2.22	2.14(5)	11(1)	6

* N_{tot} (2+4)=6 (Jahn-Teller dist.)

5. ACKNOWLEDGMENTS

This work is financially supported by the Deutsche Forschungsgemeinschaft DFG (WO882/4-2). The authors gratefully thank the XAFS beamline service group at Synchrotron Light Laboratory Elettra (XAFS Station, Trieste, Italy) for their support. We wish also to thank Mrs. G.

Arnold for her helpful work ICP-OES analysis, cerimetry) and Mr. M. Marinaro for the fruitful discussion.

6. REFERENCES

- [1] G. Arnold, J. Garche, R. Hemmer, S. Ströbele, C. Vogler, and M. Wohlfahrt-Mehrens. Fine-particle lithium iron phosphate LiFePO_4 synthesized by a new low-cost aqueous precipitation technique. *Journal of Power Sources*, 119:247–251, 2003.
- [2] G. Chen and T. J. Richardson. Solid solution phases in the olivine-type $\text{LiFePO}_4/\text{FePO}_4$ system. *Journal of the Electrochemical Society*, 156(9):A756–A762, 2009.
- [3] D. Choi, J. Xiao, Y. J. Choi, J. S. Hardy, M. Vijayakumar, M. Bhuvaneshwari, J. Liu, W. Xu, W. Wang, Z. Yang, et al. Thermal stability and phase transformation of electrochemically charged/discharged LiMnPO_4 cathode for li-ion batteries. *Energy & Environmental Science*, 4(11):4560–4566, 2011.
- [4] C. Delacourt, L. Laffont, R. Bouchet, C. Wurm, J.-B. Leriche, M. Morcrette, J.-M. Tarascon, and C. Masquelier. Toward understanding of electrical limitations (electronic, ionic) in LiMPO_4 ($m = \text{Fe}, \text{Mn}$) electrodematerials. *Journal of the Electrochemical Society*, 152(5):A913–A921, 2005.
- [5] C. Delacourt, P. Poizot, M. Morcrette, J.-M. Tarascon, and C. Masquelier. One-step low-temperature route for the preparation of electrochemically active LiMnPO_4 powders. *Chemistry of Materials*, 16(1):93–99, 2004.
- [6] C. Delacourt, P. Poizot, J.-M. Tarascon, and C. Masquelier. The existence of a temperature driven solid solution in Li_xFePO_4 for $0 < x < 1$. *Nature materials*, 4(3):254–260, 2005.
- [7] A. Di Cicco, G. Aquilanti, M. Minicucci, E. Principi, N. Novello, A. Cognigni, and L. Olivi. Novel XAFS capabilities at ELETTRA synchrotron light source. 190(1):012043, 2009.
- [8] A. Filipponi and A. Di Cicco. X-ray-absorption spectroscopy and n-body distribution functions in condensed matter. II. data analysis and applications. *Physical Review B*, 52(21):15135, 1995.
- [9] A. Filipponi, A. Di Cicco, and C. R. Natoli. X-ray absorption spectroscopy and n-body distribution functions in condensed matter. I. theory. *Physical Review B*, 52(21):15122, 1995.
- [10] O. Garcia-Moreno, M. Alvarez-Vega, F. Garcia-Alvarado, J. Garcia-Jaca, J. Gallardo-Amores, M. Sanjuan, and U. Amador. Influence of the structure on the electrochemical performance of lithium transition metal phosphates as cathodic materials in rechargeable lithium batteries: a new high-pressure form of LiMPO_4 ($M = \text{Fe}$ and Ni). *Chemistry of materials*, 13(5):1570–1576, 2001.
- [11] B. Gilbert, B. Frazer, A. Belz, P. Conrad, K. Neilson, D. Haskel, J. Lang, G. Srajer, and G. De Stasio. Multiple scattering calculations of bonding and x-ray absorption spectroscopy of manganese oxides. *The Journal of Physical Chemistry A*, 107(16):2839–2847, 2003.
- [12] J. Kim, K.-Y. Park, I. Park, J.-K. Yoo, D.-H. Seo, S.-W. Kim, and K. Kang. The effect of particle size on phase stability of the delithiated Li_xMnPO_4 . *Journal of The Electrochemical Society*, 159(1):A55–A59, 2011.
- [13] S.-W. Kim, J. Kim, H. Gwon, and K. Kang. Phase stability study of $\text{Li}_{1-x}\text{MnPO}_4$ ($0 < x < 1$) cathode for li rechargeable battery. *Journal of The Electrochemical Society*, 156(8):A635–A638, 2009.
- [14] L. Laffont, C. Delacourt, P. Gibot, M. Y. Wu, P. Kooyman, C. Masquelier, and J. M. Tarascon. Study of the $\text{LiFePO}_4/\text{FePO}_4$ two-phase system by high-resolution electron energy loss spectroscopy. *Chemistry of Materials*, 18(23):5520–5529, 2006.
- [15] S. K. Martha, O. Haik, E. Zinigrad, I. Exnar, T. Drezen, J. H. Miners, and D. Aurbach. On the thermal stability of olivine cathode materials for lithium-ion batteries. *Journal of the Electrochemical Society*, 158(10):A1115–A1122, 2011.
- [16] A. Padhi, K. Nanjundaswamy, and J. Goodenough. Phospho-olivines as positive-electrode materials for rechargeable lithium batteries. *Journal of the electrochemical society*, 144(4):1188–1194, 1997.
- [17] L. Piper, N. Quackenbush, S. Sallis, D. Scanlon, G. Watson, K.-W. Nam, X.-Q. Yang, K. Smith, F. Omenya, N. Chernova, et al. Elucidating the nature of pseudo jahn–teller distortions in Li_xMnPO_4 : Combining density functional theory with soft and hard x-ray spectroscopy. *The Journal of Physical Chemistry C*, 117(20):10383–10396, 2013.
- [18] P. P. Prosini, M. Lisi, D. Zane, and M. Pasquali. Determination of the chemical diffusion coefficient of lithium in LiFePO_4 . *Solid State Ionics*, 148(1):45–51, 2002.
- [19] T. Ressler, S. L. Brock, J. Wong, and S. L. Suib. Multiple-scattering EXAFS analysis of tetraalkylammonium manganese oxide colloids. *The Journal of Physical Chemistry B*, 103(31):6407–6420, 1999.
- [20] M. A. Roscher, J. Vetter, and D. U. Sauer. Characterisation of charge and discharge behaviour of lithium ion batteries with olivine based cathode active material. *Journal of Power sources*, 191(2):582–590, 2009.
- [21] V. Srinivasan and J. Newman. Discharge model for the lithium iron-phosphate electrode. *Journal of the*

Electrochemical Society , 151(10):A1517–A1529, 2004.

- [22] Y. Wang, P. He, and H. Zhou. Olivine LiFePO_4 : development and future. *Energy & Environmental Science*, 4(3):805–817, 2011.
- [23] A. Yamada and S.-C. Chung. Crystal chemistry of the olivine-type $\text{Li}(\text{Mny Fe}_{1-y})\text{PO}_4$ and $(\text{Mny Fe}_{1-y})\text{PO}_4$ as possible 4 V cathode materials for lithium batteries. *Journal of the Electrochemical Society* , 148(8):A960-A967, 2001.
- [24] A. Yamada, Y. Kudo, and K.-Y. Liu. Phase diagram of $\text{Li}(\text{Mny Fe}_{1-y})\text{PO}_4$ ($0 \leq x, y \leq 1$). *Journal of the Electrochemical Society* , 148(10):A1153–A1158, 2001.
- [25] A. Yamada, Y. Takei, H. Koizumi, N. Sonoyama, R. Kanno, K. Itoh, M. Yonemura, and T. Kamiyama. Electrochemical, magnetic, and structural investigation of the $\text{Li}_x(\text{Mny Fe}_{1-y})\text{PO}_4$ olivine phases. *Chemistry of materials* , 18(3):804–813, 2006.